

UNCLASSIFIED

AD NUMBER

AD859273

LIMITATION CHANGES

TO:

Approved for public release; distribution is unlimited.

FROM:

Distribution authorized to U.S. Gov't. agencies and their contractors;
Administrative/Operational Use; JUN 1969. Other requests shall be referred to Army Aviation Materiel Labs., Fort Eustis, VA.

AUTHORITY

USAAMRDL ltr 23 Jun 1971

THIS PAGE IS UNCLASSIFIED

AD 859273

AD

USAAVLABS TECHNICAL REPORT 69-54

INVESTIGATION OF FACTORS AFFECTING SMALL TURBINE EFFICIENCY AND LOSS PREDICTION

FINAL REPORT

By
LeRoy T. Burrows

June 1969

U. S. ARMY AVIATION MATERIEL LABORATORIES
FORT EUSTIS, VIRGINIA

This document is subject to special export controls and each transmittal to foreign governments or foreign nationals may be made only with prior approval of US Army Aviation Materiel Laboratories, Fort Eustis, Virginia 23604.



SEP 25 1969

DISCLAIMERS

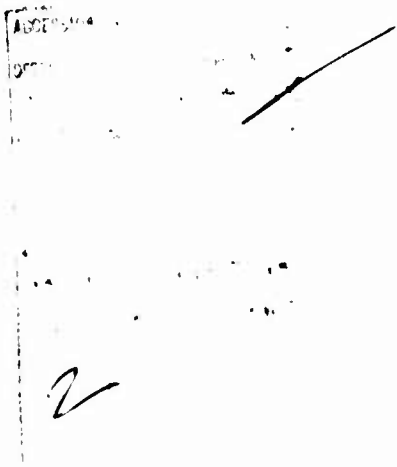
The findings in this report are not to be construed as an official Department of the Army position unless so designated by other authorized documents.

When Government drawings, specifications, or other data are used for any purpose other than in connection with a definitely related Government procurement operation, the United States Government thereby incurs no responsibility nor any obligation whatsoever; and the fact that the Government may have formulated, furnished, or in any way supplied the said drawings, specifications, or other data is not to be regarded by implication or otherwise as in any manner licensing the holder or any other person or corporation, or conveying any rights or permission, to manufacture, use, or sell any patented invention that may in any way be related thereto.

Trade names cited in this report do not constitute an official endorsement or approval of the use of such commercial hardware or software.

DISPOSITION INSTRUCTIONS

Destroy this report when no longer needed. Do not return it to the originator.



Task 1G162203D14413
USAAVLABS Technical Report 69-54
June 1969

INVESTIGATION OF FACTORS AFFECTING
SMALL TURBINE EFFICIENCY AND LOSS PREDICTION

Final Report

By

LeRoy T. Burrows

U. S. ARMY AVIATION MATERIEL LABORATORIES
FORT EUSTIS, VIRGINIA

This document is subject to special export controls
and each transmittal to foreign governments or foreign
nationals may be made only with prior approval of US Army
Aviation Materiel Laboratories, Fort Eustis, Virginia 23604.

SUMMARY

The aerodynamics and mechanics of the high-temperature, low-mass-flow, low-aspect-ratio, axial-flow turbine are discussed. The problems of small size and resulting high secondary losses are considered, and approaches to improving efficiency are offered. In addition, experimental analysis of a turbine stator annulus (aspect ratio = 0.5) is presented, with recommendation for an accurate prediction of the losses in the small, high-performance turbine.

FOREWORD

The work described in this report was conducted while the author was a student at the Von Kármán Institute for Fluid Dynamics (VKI), Rhode-Saint-Genese, Belgium. Guidance and assistance from Professor J. Chauvin and other staff and laboratory personnel of the institute contributed greatly to this investigation.

The full-scale turbine stator annulus test model was fabricated by Continental Aviation and Engineering Corporation (CAE) under Contract DA 44-177-AMC-184(T) as part of the Army's advanced turbine component program. Assistance from Mr. Cass Rogo, CAE, in obtaining this model and its specifications is gratefully acknowledged.

The work reported herein was authorized by DA Task 1G162203D14413.

TABLE OF CONTENTS

	<u>Page</u>
SUMMARY	iii
FOREWORD	v
LIST OF ILLUSTRATIONS	viii
LIST OF SYMBOLS	ix
INTRODUCTION.	1
THE SMALL TURBINE DESIGN PROBLEM	3
Mechanical Design Considerations	3
Aerodynamic Design for Maximum Efficiency	5
TURBINE LOSS PREDICTION	13
Stator Model Design Description	13
Stator Loss Analysis	13
EXPERIMENTAL INVESTIGATION OF THE PERFORMANCE OF A LOW-ASPECT-RATIO TURBINE STATOR ANNULUS . . .	22
Description of Test Apparatus.	22
Test Procedure	24
Discussion of Results	26
Comparison of Experimental and Theoretical Losses	29
LITERATURE CITED.	30
DISTRIBUTION	32

LIST OF ILLUSTRATIONS

<u>Figure</u>		<u>Page</u>
1	Continental Turbine Flow Path	2
2	Stress Rupture Properties.	4
3	Turbine Loss Components	6
4	Secondary Flows in a Turbine Cascade	7
5	Boundary Layer Interaction in a Stator Blade Row	7
6	Meridional Constriction.	10
7	Profile Velocity Distribution With and Without Meridional Constriction.	11
8	Ainley's Loss Correlation	16
9	Ainley's Loss Correlation	16
10	Ainley's Loss Correlation	16
11	Soderberg's Loss Correlation	17
12	Stator Nozzle Test Model	23
13	Stator Nozzle Test Model	23
14	Stator Nozzle Test Rig	24
15	Stator Nozzle Test Rig	25
16	Stator Nozzle Test Probes.	26
17	Stator Nozzle Outlet Loss Distribution	27
18	Radial Variation in Stator Nozzle Loss	27
19	Variation of Stator Nozzle Outlet Angle	28

LIST OF SYMBOLS

A	area, in.²
A_N	annulus area, in.²
b	axial chord, in.
C	chord, in.
c	absolute velocity, ft/sec
C_L	lift coefficient
c_x, c_y, c_r, c_θ	components of absolute velocity, ft/sec
c_p	specific heat at constant pressure, Btu/lb °F
c_v	specific heat at constant temperature, Btu/lb °F
H	blade or vane height, in.
ΔH	turbine work, Btu/lb or ft²/sec²
i	incidence angle, deg
LER	leading edge radius, in.
M	Mach number
N	rotative speed, rpm
P₀	stagnation pressure, psia
p	static pressure, psia
R	reaction, %
Re	Reynolds number based on chord and exit velocity
R_h	Reynolds number based on hydraulic diameter

r	radius, in.
s	spacing, in.
T_0	stagnation temperature, °F or °R
T	static temperature, °F or °R
t	vane mean thickness, in.
TER	trailing edge radius, in.
TET	trailing edge thickness, in.
U	blade speed, ft/sec
w_g	gas flow rate, lb/sec
w	relative velocity, ft/sec
$w_x, w_y,$ w_r, w_θ	components of relative velocity, ft/sec
Y	loss coefficient (Ainley)
α	absolute flow angle, deg
β	relative flow angle, deg
γ	ratio of specific heat
ϵ	deflection, deg
$\eta_{T,T}$	total-to-total adiabatic efficiency, %
θ	camber, deg
ξ	loss coefficient (Soderberg)
$\bar{\xi}$	loss coefficient (Markov)
ρ	density, lb/ft
σ	centrifugal tensile stress, ksi = psi $\times 10^3$

δ	stagger, deg
\bar{c}	loss coefficient

SUBSCRIPTS

1	entry to stator nozzle
2	stator nozzle exit or rotor entry
3	exit from rotor
m	mean
0	stagnation conditions
N	nozzle
t	throat
REL	relative conditions
ψ, θ	tangential
x	axial
r	radial
p	profile
s	secondary
TE	trailing edge

BLANK PAGE

INTRODUCTION

V/STOL aircraft mission requirements have placed increasing importance on the development of advanced small gas turbine engines (500 to 1500 shp) with high power-to-weight ratio, low specific fuel consumption, and low installed volume. Significant increases in engine performance must of course be preceded by technology advancements in the compressor, combustor, and turbine components.

The U. S. Army Aviation Materiel Laboratories initiated a small gas turbine component technology program in 1964 with the long-range purpose of demonstrating an engine technology which, with respect to the then-existing state of the art, would provide twice the specific horsepower with significant reductions in envelope and specific fuel consumption.¹ As a part of this program, two advanced turbine efforts were funded for design, fabrication, and experimental testing: a fluid-cooled concept proposed by Continental Aviation and Engineering Corporation, and a transpiration-cooled design offered by Curtiss-Wright Corporation. Consistent with the overall engine design objectives from cycle analyses given in Reference 1, the specific objectives for the single-stage axial fluid-cooled gasifier turbine were:

Turbine inlet temperature	2300° to 2500°F
Total-to-total adiabatic efficiency	86.5%
Airflow	5 lb/sec
Inlet pressure ratio	8.6
Rotative speed	50,000 rpm
Turbine work	138 Btu/lb

The objectives of the transpiration-cooled design were about the same except for a proposed efficiency of 90%. Some flow path dimensions of the fluid-cooled design are given in Figure 1. Although effective cooling was generally considered to be the difficult task for these programs, the most elusive objective was the predicted efficiency. In fact, neither contractor demonstrated an efficiency greater than 80%. One cannot accept this level of efficiency for an axial turbine when consideration is given to the effect on engine performance and to the competitive status of the radial inflow turbine for the small turbine application.

It is therefore the intent here to investigate both the aerodynamics and the mechanics of the small, high-pressure-ratio, axial-flow gasifier turbine, with emphasis on improving efficiency. The problems associated with

small size are discussed, and approaches to improving efficiency are offered. In addition, a turbine stator designed and fabricated by Continental² was tested at VKI; the results are presented herein and are compared to the existing loss criteria.

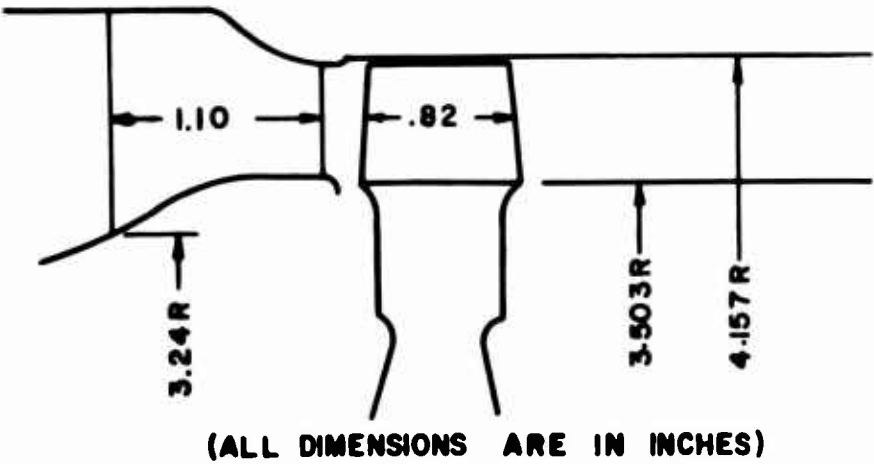


Figure 1. Continental Turbine Flow Path.

THE SMALL TURBINE DESIGN PROBLEM

The advanced small gas turbine is characterized by high gas temperatures, low mass flows, and high pressure ratios; and, to achieve the desired performance gains, it must have good efficiency. The combination of small size and high temperature presents difficult mechanical problems that can influence the turbine design to such an extent as to make the difficult aerodynamic design problem an impossible one. Therefore, to satisfy both reliability and performance criteria, the designer is faced with judicious trade-offs to ensure a design that is suitable both mechanically and aerodynamically.

MECHANICAL DESIGN CONSIDERATIONS

For the high-temperature (2300° to 2500°F) turbine, stress and cooling considerations greatly influence the design. User requirements for long design life and time between overhaul place emphasis on reduction of rotor blade stresses and material temperatures.

Centrifugal stresses may be reduced by minimizing blade speed, maximizing hub-tip ratio, and tapering the blade; however, the designer will find that these approaches are not completely compatible with an aerodynamic requirement for reasonably sized flow channels. This is an example of one of the trade-offs required. High centrifugal tensile stress levels at design temperature are inevitable, thus dictating stringent blade cooling requirements. An example of this relationship can be seen in Figure 2, which shows stress rupture properties that are typical of the best existing high-strength cast nickel-base alloys. For the high rotative speeds associated with small turbines (40,000 to 60,000 rpm), centrifugal stresses in the order of 35,000 to 78,000 psi are common. At these stress levels for a 1000-hour stress-rupture life at a design gas temperature of 2300° or 2500°F, the rotor blades must be cooled to approximately 1500° to 1600°F.

This example is a simplified illustration of the magnitude of the cooling requirement. In reality, the designer must consider, in addition to the centrifugal stress:

1. The thermal stress arising from variations in chordwise temperature
2. Thermal fatigue from cyclic changes in operating temperature

3. Percentage of operation at design and off-design temperatures
4. The average temperature seen by the blade both chordwise and spanwise

The installation of cooling systems inside vanes and blades 0.5 to 1.0 inch in height presents a difficult fabrication problem and is not conducive to good cooling efficiency. Although the surface to be cooled is small, so is the available cooling flow. In the small, compact engine, the distance between the combustor and the turbine will be short; and the resulting severe radial and circumferential temperature distributions seen by the stator must be accounted for in the cooling design.

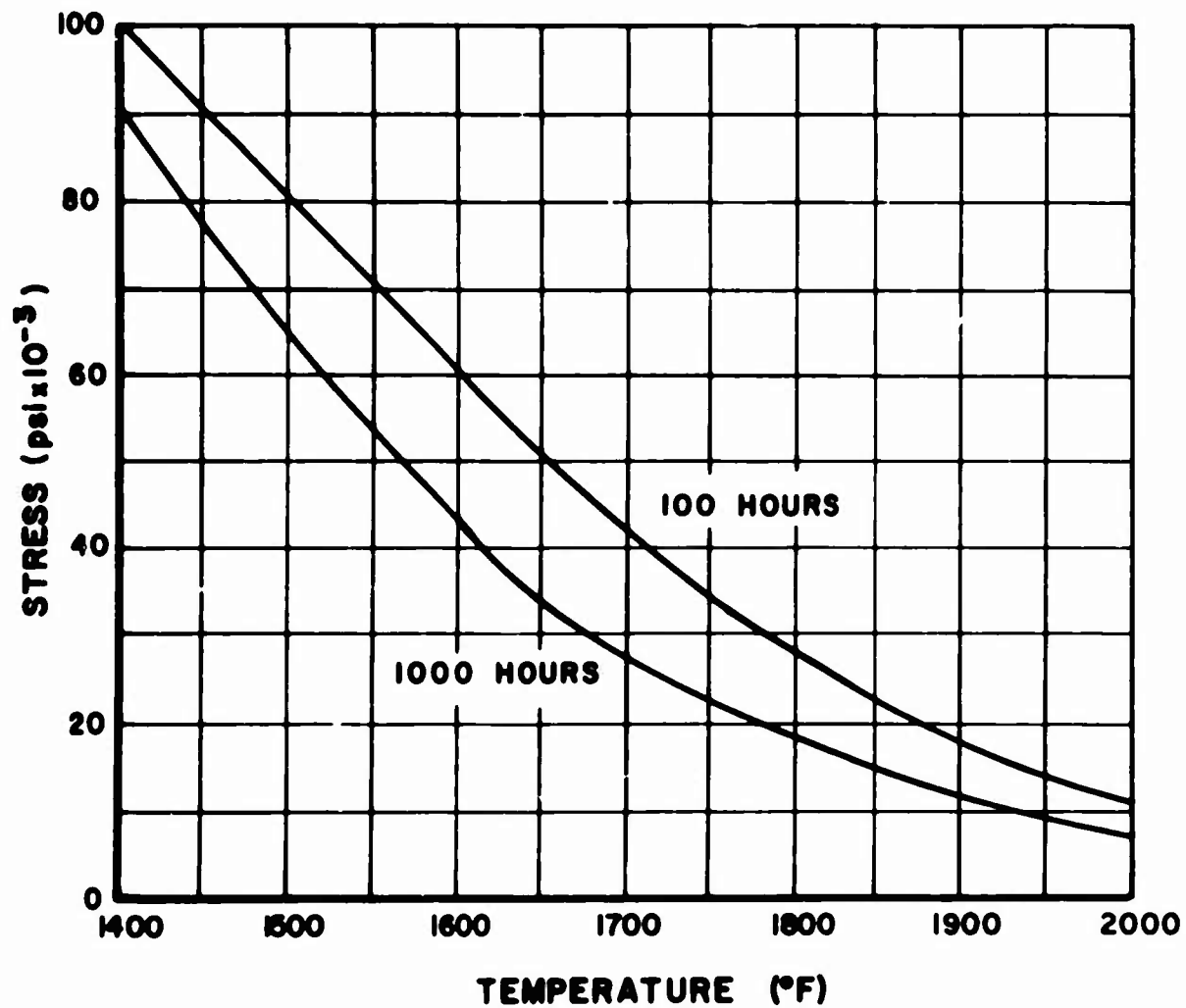


Figure 2. Stress Rupture Properties.

AERODYNAMIC DESIGN FOR MAXIMUM EFFICIENCY

The aerodynamic design considerations of the advanced small gas turbine are unique because of the small size and high loadings. It shall be the intent here to define the aerodynamic efficiency problem of the small turbine and to offer potential solutions.

Problem Definition

Conditions for efficient design of a turbine may be simply stated as:

1. Moderate to subsonic velocities throughout the nozzle and rotor blading
2. Positive reaction in the nozzle and rotor blading at all radial stations
3. Low gas turning angles

However, obtaining the desired state-of-the-art gains in performance is not so simple. The combination of small size, high loadings, and increased mechanical problems will have the effect of reducing the maximum efficiency attainable for the small gasifier turbine. For example, low blade heights evolve from a combination of high pressure ratio and low mass flow, while minimum blade chord is dictated by fabrication techniques, cooling requirements, gas turning requirements, and mechanical considerations. This combination of low blade height and moderate chord length results in aspect ratios in the order of .4 to .8, which characteristically have high secondary flow losses and high tip clearance losses. In addition, increased loading gives higher profile losses, and trailing edge losses are high because of the thickness imposed by cooling requirements. Blade cooling will also require thicker leading edges and mid-sections, thus compromising optimum profile design.³

Figure 3a represents the loss breakdown in an axial-flow gasifier turbine stage for a current engine in the 1000-shp size. Figure 3b represents an advanced gasifier turbine also for a 1000-shp engine but one that is about one-half the size of the present design. Comparison of these figures indicates that:

1. Profile losses differ very little.
2. Trailing edge and tip clearance losses are moderately higher in the advanced design.
3. Secondary losses are significantly greater in the advanced design.

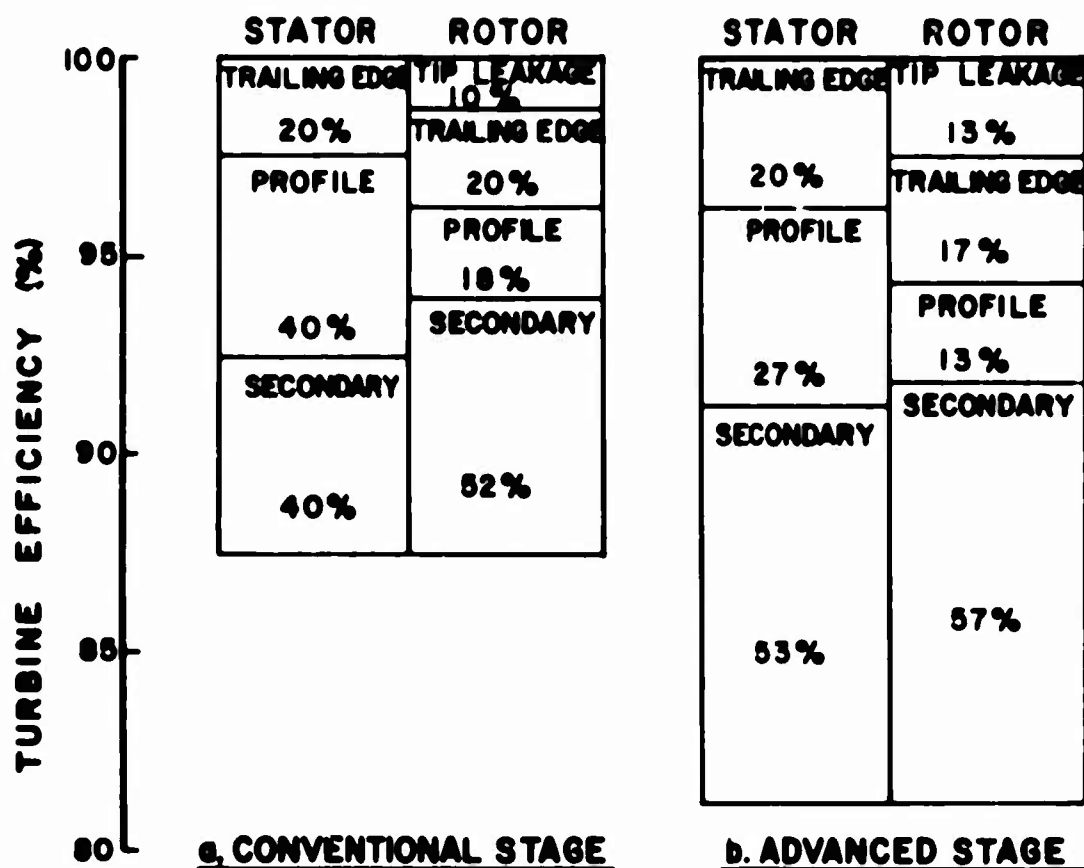


Figure 3. Turbine Loss Components.

Significant reductions in tip leakage and trailing edge thickness are mechanical problems and do not appear to be likely. New techniques for minimizing tip clearance and special cooling methods to reduce trailing edge thickness could in the future provide some measure of improvement here. However, meaningful improvements in efficiency must correspond to a reduction in secondary flows and/or their effects.

Secondary Flows and Losses

The most important secondary flows are those created when the boundary layer on the annulus walls is deflected through the blade row, creating a component of vorticity along the stream direction (Figures 4 and 5). In a blade row, losses result from a combination of viscous dissipation of the induced secondary velocities and separation of the boundary layer in the corner between the annulus wall and the profile suction surface. In the rotor, the flow pattern is complicated by the scraping vortex at the blade tip, by leakage flows, by radial flows, and by the influence of the upstream secondary flows. In the rotor, the unloading of the blade at the tip constitutes a fair portion of the total secondary losses.⁴ Other secondary flows

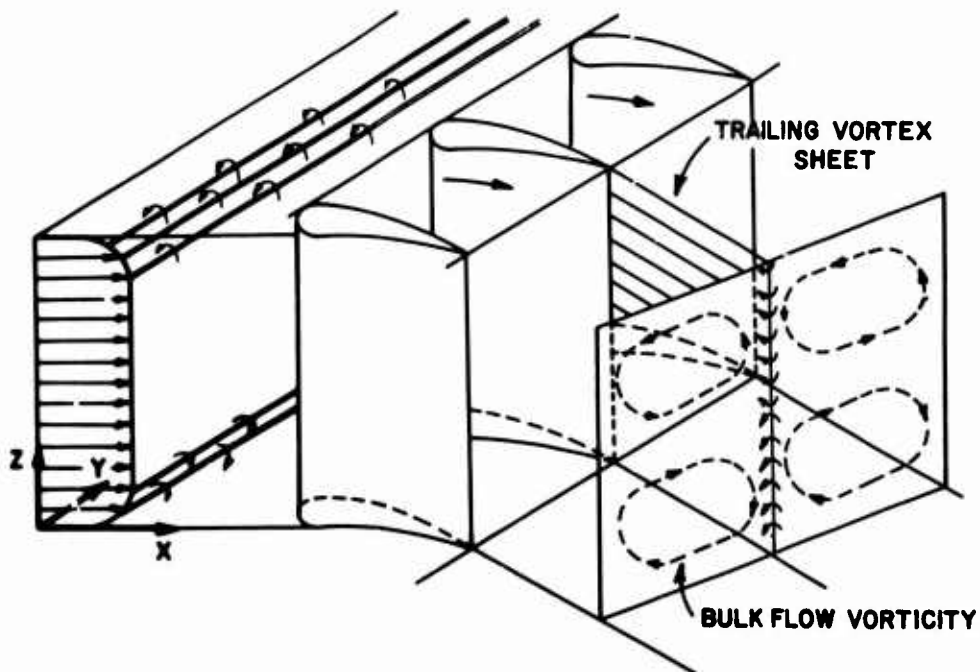


Figure 4. Secondary Flows in a Turbine Cascade.

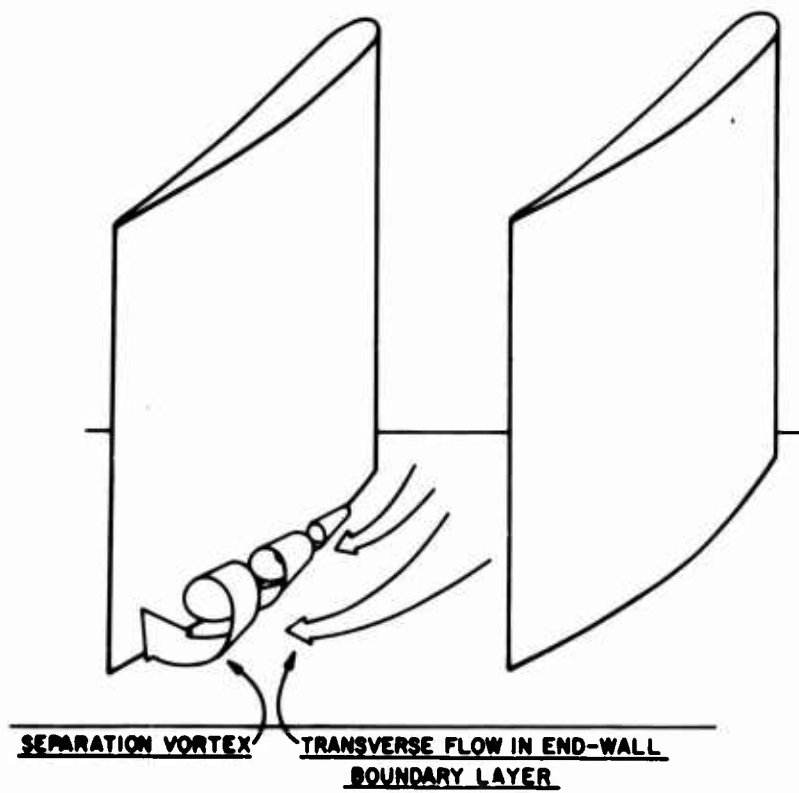


Figure 5. Boundary Layer Interaction in a Stator Blade Row.

are created by a trailing filament vorticity transmitted from upstream and a shed vorticity resulting from the change of lift along the blade; however, these effects are generally small.

Numerous empirical and semiempirical relationships have been used to evaluate the secondary losses in blade rows, with most being based on rectilinear cascade data. In the rectilinear cascade, the regions of high loss are disposed symmetrically over the height; while in an annular cascade, there is a nonsymmetrical distribution of the eddy regions, and the losses in the root sections are somewhat higher than those in the tip sections. As a result, total losses in the annular cascade are greater than those in the straight cascade. Most analytical approaches to the problem assume incompressible, inviscid flow and neglect the centrifugal effects due to rotation. Very little is known about the interaction of leakage, radial flows, and scraping vorticities with mainstream secondary flows. It is not the intent to analyze the expressions for secondary loss here, although in a later section of this report a number of them are compared with experimental results of a three-dimensional annular cascade.

It is generally conceded that aspect ratio is important in determining secondary losses, since end-wall boundary layer thickness is a function of chord length and since, as blade height is reduced, the influence of the secondary flows on the total flow increases. In fact, New⁵ published experimental cascade data indicating that, for a given chord, the secondary loss might be inversely proportional to the blade height.

Reduction of Secondary Loss

Two approaches to increasing turbine efficiency through the reduction of secondary loss are the reduction of secondary flows and the reduction of secondary flow effects.

The reduction of secondary flows may be accomplished by minimizing

1. Gas deflections
2. Tip leakage
3. Radial flows in the rotor
4. Radial pressure gradient in the stator
5. End-wall boundary layer thickness
6. Difference in pressure between the concave and convex surfaces in the flow channel

The high stage work requirement for advanced small turbines requires the use of high deflections and high profile lift coefficients, while mechanical considerations limit the minimum tip clearance possible. Radial flows in the rotor and the stator radial pressure gradient may be reduced by tilting⁶ the vanes or blades with respect to a radial line normal to the wheel axis, although the practicality of this approach has not been established. Reduction of end-wall boundary layer thickness could be achieved by

1. Minimizing chord length
2. Minimizing upstream boundary layer thickness
3. Accelerating the boundary layer in the meridional plane

As said before, the minimum blade chord is dictated by mechanical considerations and gas turning requirements, neither of which can be reduced significantly. Avoidance of any significant boundary layer accumulation in the channel between the combustor and the turbine represents good design practice. This would imply that in the small turbine, film cooling of the annulus walls by air injection upstream of the stator may increase the boundary layer thickness, thereby reducing performance. On the other hand, it is possible that selective positioning of cooling air injection in the stator flow channel could result in acceleration of the end-wall boundary layer impeding the boundary layer's transport from the pressure to the suction side.

Meridional constriction is a good method for reducing secondary loss in turbine stages with short blades; that is, the profiling of the stator annulus walls in the flow channel. Since the stator exit flow angle and area are fixed by velocity triangle and continuity requirements, constriction will require an increase in the vane height at the stator entrance (Figure 6). Profiling of the channels over the height attacks the secondary flow problem in the following ways:⁷

1. Reduction of the velocity on the sections of maximum curvature of the channel, where secondary flow effects are intensive, results in an increase in the pressure on the profile suction surface and a corresponding decrease in the difference in pressures between the suction and pressure surfaces of the flow channel (Figure 7).
2. Convergence of the flow in the oblique cut (i. e., in the area behind the most curved section of the channel) decreases the thickness of the boundary layer at the end walls, thus leading to a reduction in the intensity of the secondary flow.

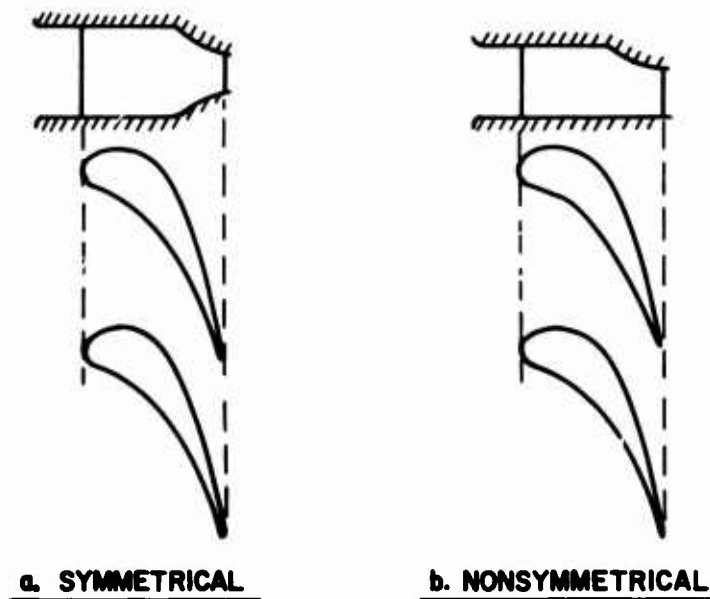


Figure 6. Meridional Constriction.

Two general types of meridional constriction are considered:

1. Symmetrical constriction with straight or curved tapers (Figure 6a)
2. Nonsymmetrical constriction (Figure 6b)

Symmetrical constriction with convergence at both walls offers the best approach to the reduction of secondary flows. However, nonsymmetrical constriction makes possible the solution of two problems - reduction of secondary loss, and reduction of the radial pressure gradient - thus providing constant reaction along the radius.

The advanced compact turbine requires a highly loaded initial stage and accompanying high deflections. Here, again, the use of meridional constriction is advantageous. Figure 7 illustrates typical velocity distributions for an NACA primary turbine series profile and a profile with meridional constriction, both for 75 degrees deflection. Turbine blade loading limits suggested by Stewart⁸ based on diffusion factors indicate that the profile with meridional constriction offers the optimum velocity distribution. It may be concluded that from a limit loading standpoint, shorter chords could be obtained using meridional constriction.

It is appropriate here to point out that aerodynamically ideal profiles are required to obtain maximum efficiencies. Existing turbine profile series may not be adequate for use in a design using meridional constriction.

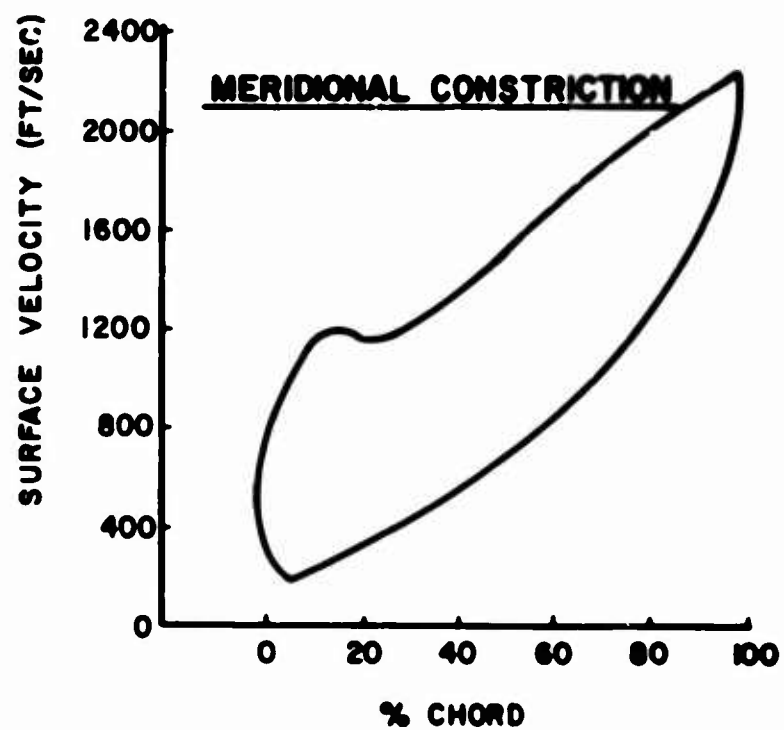
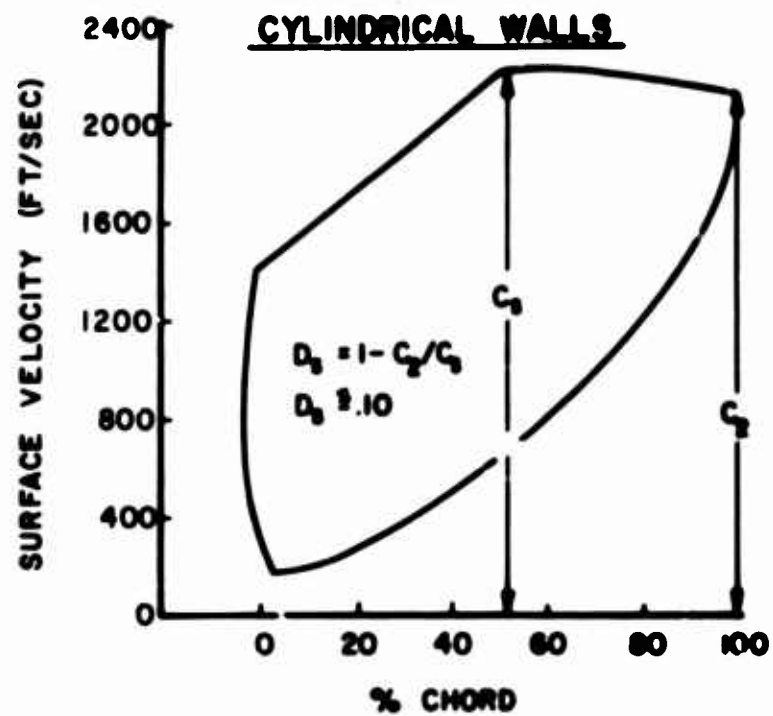


Figure 7. Profile Velocity Distribution With and Without Meridional Constriction.

Although meridional constriction is, strictly speaking, applicable only to the stator, it is possible that the rationale may be applied to the rotor by incorporating convergent-divergent channels. The application of controlled vortex aerodynamics to rotor design also has the potential for reduction of secondary flows, in that constant reaction over the span is possible. Conventional methods for satisfying radial equilibrium requirements result in large variations of reaction.

A reduction of secondary flow effects can be accomplished by designing to obtain the greatest blade heights possible. This will require trade-offs not normally considered in a turbine design effort.

TURBINE LOSS PREDICTION

Prediction of losses in low-aspect-ratio turbine blade rows has been difficult because of the inability of designers to accurately account for secondary losses and trailing edge thickness losses. The objective of this study is to analyze various existing loss prediction methods and their components, to compare these methods, and then to define a method suitable for predicting losses in a low-aspect-ratio turbine. A turbine stator was used as a model for analysis, and it is described below.

STATOR MODEL DESIGN DESCRIPTION

Number of vanes	17
Average blade height, H_{avg}	0.857 in.
Minimum blade height, H_{min}	0.564 in.
Chord, C	1.637 in.
Axial chord, b	1.100 in.
Inlet flow angle, α_1	0 deg
Exit flow angle, α_2	70 deg
Inlet annulus area, A_{N1}	27.594 in. ²
Exit annulus area, A_{N2}	13.519 in. ²
Throat area, A_t	4.63 in. ²
Leading edge radius, LER	0.08 in.
Trailing edge radius, TER	0.025 in.

STATOR LOSS ANALYSIS

Three methods of predicting the total loss of a stationary turbine blade row are those offered by Ainley, Soderberg, and Markov. It is possible to

divide these total loss coefficients into components of profile and secondary and trailing edge thickness losses. These loss coefficients are defined as:

$$\xi = \frac{h_2 - h_{2s}}{h_{01} - h_2} \quad \text{loss coefficient (Soderberg)}$$

$$\bar{\xi} = \frac{h_2 - h_{2s}}{\frac{1}{2} c_{2s}^2} \quad \text{loss coefficient (Markov)}$$

$$Y = \frac{P_{01} - P_{02}}{P_{02} - p_2} \quad \text{loss coefficient (Ainley)}$$

where h = enthalpy
 subscript s = at end of isentropic expansion

These loss coefficients can be related by

$$\bar{\xi} = \frac{\xi}{1 + \xi}$$

$$Y = \xi \left(1 + \frac{\gamma M_2^2}{2} \right) \quad \text{for } M_2 < 1$$

A description of these loss correlations and additional references can be found in Reference 9. Ainley's and Soderberg's methods are empirical in nature, while Markov bases his method on boundary layer development with an empirical expression for secondary loss. Stator model loss is predicted by each of these methods as follows:

Mean thickness/chord ratio, t/C	0.20
Spacing/chord ratio, s/C	0.855
Spacing, s	1.399 in.
Deflection, ϵ	70 deg
Stagger, ψ	50° 61'

Incidence, i	0
Mach number at exit, M_2	1.0

The stator vanes are of constant cross section and incorporate meridional constriction.

Ainley's Method¹⁰

This method is based on test results, and the losses are calculated using a series of graphical correlations, which are repeated in this report as Figures 8, 9, and 10. These figures are based on zero incidence, $t/C = 20\%$, and $Re = 2 \times 10^5$, which are consistent with model stator design. However, the correlation figures are based on low-speed data ($M_2 < 0.6$), which is not the case for the model. The loss may be calculated with this method as follows:

for $i = 0$ and $\frac{t}{C} = .20$,

$$Y_p = \left[Y_{p(\alpha_1 = 0)} + \left(\frac{\alpha_1}{\alpha_2} \right)^2 (Y_{p(\alpha_1 = \alpha_2)} - Y_{p(\alpha_1 = 0)}) \right] = .041$$

where $Y_{p(\alpha_1 = 0)}$ is obtained from Figure 8

$Y_{p(\alpha_1 = \alpha_2)}$ is obtained from Figure 9

$$Y_s = \lambda \left(\frac{C_L}{s/C} \right)^2 \frac{\cos^2 \alpha_2}{\cos^3 \alpha_m} = .033$$

where $\lambda = f \left[\frac{(A_2/A_1)^2}{1 + \frac{I.D.}{O.D.}} \right] = .0055$ from Figure 10

$$\frac{C_L}{s/C} = 2(\tan \alpha_1 - \tan \alpha_2) \cos \alpha_m = 3.23$$

$$\alpha_m = \tan^{-1} \left(\frac{\tan \alpha_1 + \tan \alpha_2}{2} \right) = 54^\circ$$

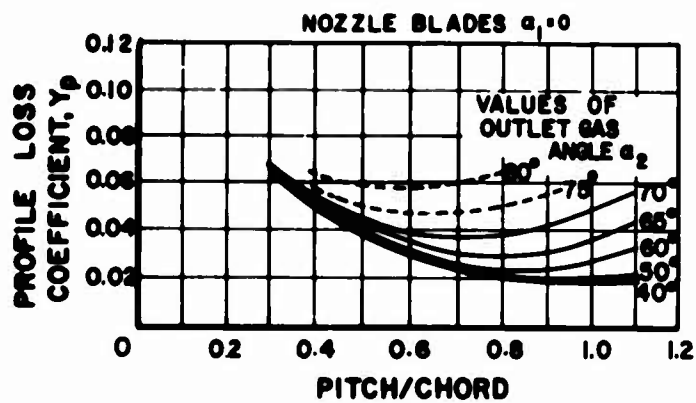


Figure 8. Ainley's Loss Correlation.

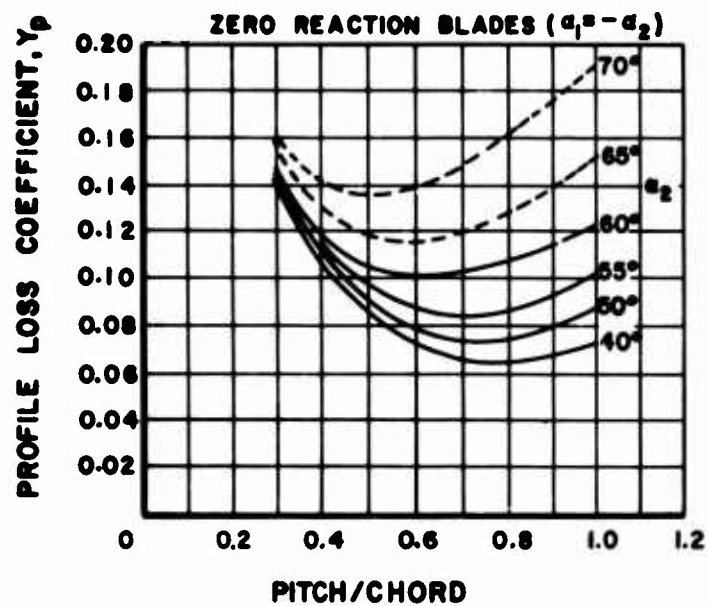


Figure 9. Ainley's Loss Correlation.

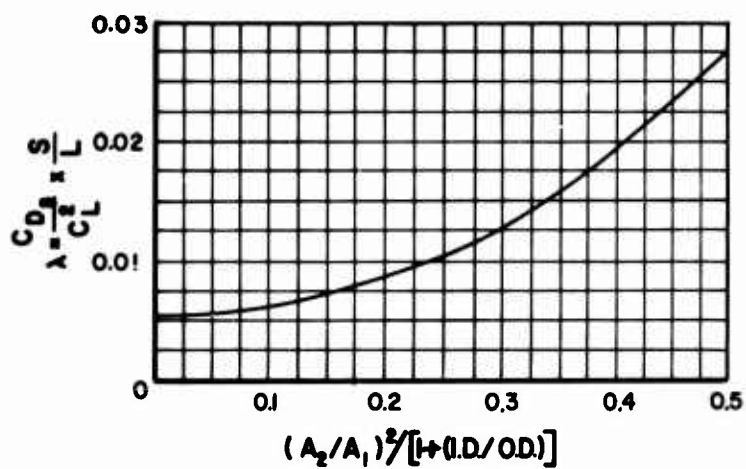


Figure 10. Ainley's Loss Correlation.

The profile loss can then be corrected for trailing edge thickness by

$$Y_{pc} = Y_p [1 + 7(TET - 0.02)] = .0496$$

and

$$Y = Y_{ps} + Y_s = .0826 = \text{total loss}$$

Soderberg's Method⁹

This method, based on high-speed test data, does not include a specific correction for trailing edge thickness.

$$\xi = \left(\frac{10^5}{R_h} \right)^{1/4} \left[(1 + \xi') \left(0.975 + 0.075 \frac{b}{H} \right) - 1 \right] = 0.115$$

where R_h = Reynolds number based on hydraulic diameter

ξ' = nominal loss coefficient based on aspect ratio of 3
and $R_h = 1 \times 10^5$. This is obtained from Figure 11 of this report, which is repeated from Reference 9.

$H = H_{avg}$ for this design

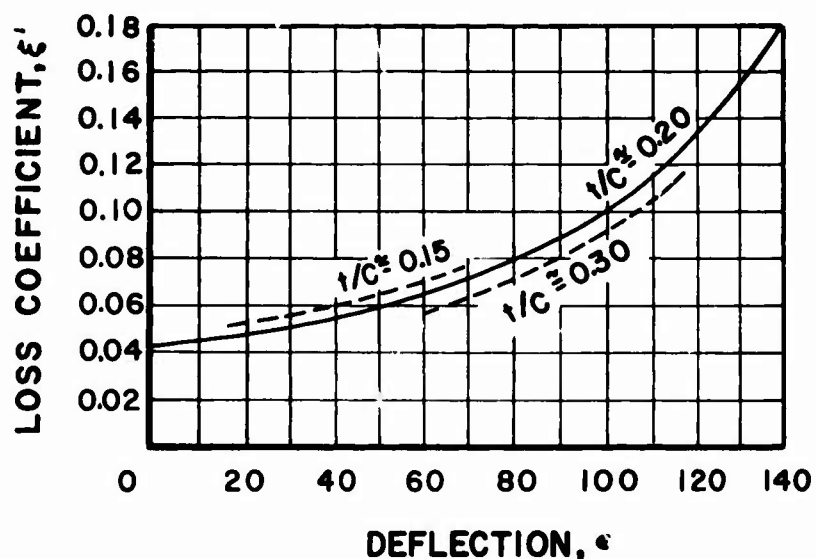


Figure 11. Soderberg's Loss Correlation.

Markov's Method⁹

$$\bar{\xi} = \bar{\xi}_p + \bar{\xi}_s$$

where $\bar{\xi}_p = \bar{\xi}_{\text{friction}} + \bar{\xi}_{\text{TE}} = \text{2-D loss}$

$$\bar{\xi}_{\text{TE}} = 0.41 \left[\frac{(\text{TET} - \text{TET}_{\text{nominal}})}{s \cos \alpha_2} \right] = .0257$$

where $\text{TET}_{\text{nominal}}$ is assumed as .020

$$\bar{\xi}_s = \frac{\bar{\xi}_{\text{wall}}}{\frac{H}{t}} = .0802$$

where $\bar{\xi}_{\text{wall}} = 0.07 \text{ to } 0.18$, with high values corresponding to low reaction, and $\bar{\xi}_{\text{wall}} = .125$ is assumed.

$$H = H_{\text{avg}}$$

$$t = \text{throat width} = 0.550 \text{ in.}$$

Not having velocity distributions to calculate friction loss, it shall be assumed that Y_p from Ainley's method is similar to $\bar{\xi}_{\text{friction}}$, or using the loss coefficient conversions,

$$\bar{\xi}_{\text{friction}} = .0242$$

is equivalent to

$$Y_p = .041$$

Then

$$\bar{\xi} = .1301$$

Comparing these total loss predictions in terms of loss coefficient, ξ , it can be seen that discrepancies exist for

Ainley $\xi = .0495$

Soderberg $\xi = .115$

Markov $\xi = .150$

Also, in comparing these results, one must consider that:

1. Ainley's method is based on low-speed test data.
2. Ainley's secondary loss expression appears not to be capable of handling very low aspect ratios.
3. Ainley's correlation for trailing edge thickness appears to be surprisingly low compared to that offered by Markov.
4. Soderberg's method is based on high-speed test data and does not include the effect of trailing edge thickness.
5. Markov's method indicates that for TET = .050 in., the TET loss may be equal to the profile friction loss.
6. Markov's loss would be close to Soderberg's loss if a value of ξ_{TET} were added.
7. Secondary loss expressions that take into account only the loss due to the dissipation of the induced secondary velocities are not adequate for low-aspect-ratio turbines.
8. Horlock states that Soderberg distributes the loss fairly evenly between rotor and stator, while Ainley assigns a much greater loss to the rotor.

Based upon the preceding analysis, it was concluded that Soderberg's correlation corrected for trailing edge loss may provide a reasonable loss prediction.

$$\xi_{total} = \xi + \xi_{TET} = .115 + .0264 = .1414$$

where ξ_{TET} is converted from Markov's expression and is approximately 20% of total loss.

$$\xi_{total} = .1414 \text{ is equivalent to } Y = .233.$$

The above-selected prediction also deviates from Soderberg's basic correlation with respect to Reynolds number correction. According to Kearton and others, cascade losses do not change significantly with increasing hydraulic Reynolds number above a value of 1×10^5 . Since the hydraulic Reynolds number of the stator model was greater than 1×10^5 , no correction was applied; however, if this value had been less than 1×10^5 , then the following correction would apply:

$$\xi_{final} = \left(\frac{10^5}{R_h} \right)^{1/4} \xi$$

It should be pointed out that the end-wall constriction of the model has been reflected in the preceding loss analysis only by H_{avg} . The loss analysis methods discussed here were not based on models incorporating end-wall profiling.

In the analysis of the small turbine, the accurate prediction of the secondary loss is the primary factor in determining the actual loss. In addition to loss expressions already given, it is worthwhile to present some other secondary loss expressions and to make comments relative thereto.

$$1. \quad \bar{\xi}_s = .01 \frac{\cos \alpha_2}{\cos \alpha_1} (\tan \alpha_2 + \tan \alpha_1) \dots \quad \text{this expression by}$$

Markov should be used only for aspect ratios greater than 2.0.

$$2. \quad \xi_s = \frac{\xi_{wall}}{\frac{H}{C}} \dots \quad \text{suggested by Scholtz, this provides losses}$$

similar to Markov's expression for low aspect ratios and appears to be reasonable.

3. $C_{D_s} = \frac{0.04 C_L^2}{\frac{H}{C}}$. . . suggested by Vavra, this gives extremely high loss for the stator model and is therefore not considered to be adequate for the very small turbine.

4. $C_{D_s} = \frac{0.12 \epsilon^2}{\left(\frac{H}{s}\right) \left(1 - \frac{0.2}{\frac{H}{s}}\right)}$. . . this expression by Ehrich and Detra

and all other expressions involving the term ϵ are good only for very small deflections.

EXPERIMENTAL INVESTIGATION OF THE PERFORMANCE OF A LOW-ASPECT-RATIO TURBINE STATOR ANNULUS

The purpose of this experimental investigation was to:

1. Determine the losses of a highly loaded, low-aspect-ratio turbine stator annulus.
2. Compare these losses to those predicted analytically by available two-dimensional loss correlation methods.
3. Determine a method suitable for predicting losses in the small advanced turbine.

This was accomplished by testing a full-scale turbine stator annulus fabricated as part of the Army's advanced turbine component program. Figures 12 and 13 provide a general picture of the model. Pertinent design data are given in the preceding section of this report and are based on the design conditions given in the Introduction.

DESCRIPTION OF TEST APPARATUS

The stator annulus was tested in the blowdown cascade tunnel (C-2) located in the VKI Turbomachinery Laboratory and pictured in Figure 14. The test model was housed in a specially designed rig, which can be seen in Figure 14 and which is shown in detail in Figure 15. Salient features of this rig include:

1. Provision for rotation of the test annulus through a 60-degree arc to permit traverse measurements in the circumferential plane.
2. Inlet lip and nose fairing included for uniform inlet flow conditions.
3. Six circumferential probe positions provided, three upstream and three downstream.
4. Window incorporated to permit observation of exit flow from model.

Five probes were used in the test. These are shown in Figure 16 and are described as follows from left to right:

1. Upstream total and directional (left-right) pressure.
2. Upstream static pressure.

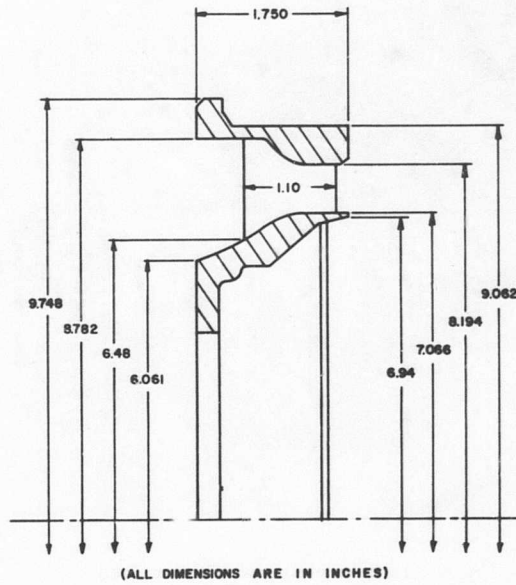


Figure 12. Stator Nozzle Test Model.

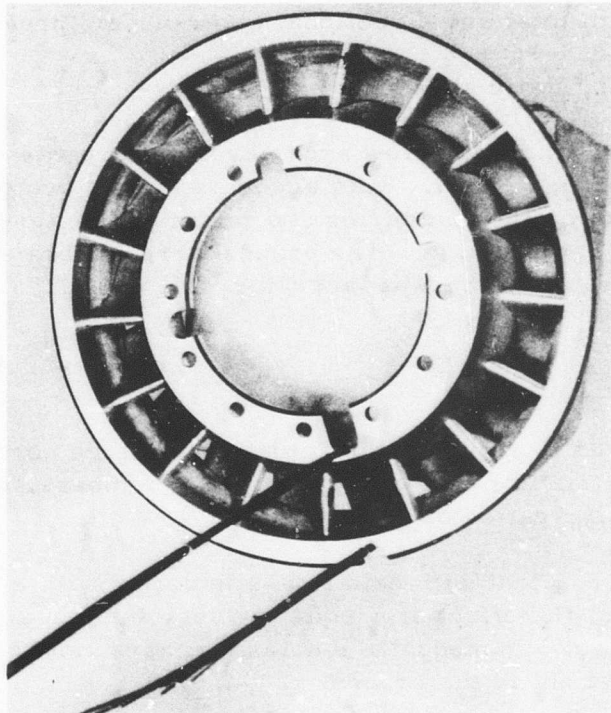


Figure 13. Stator Nozzle Test Model.

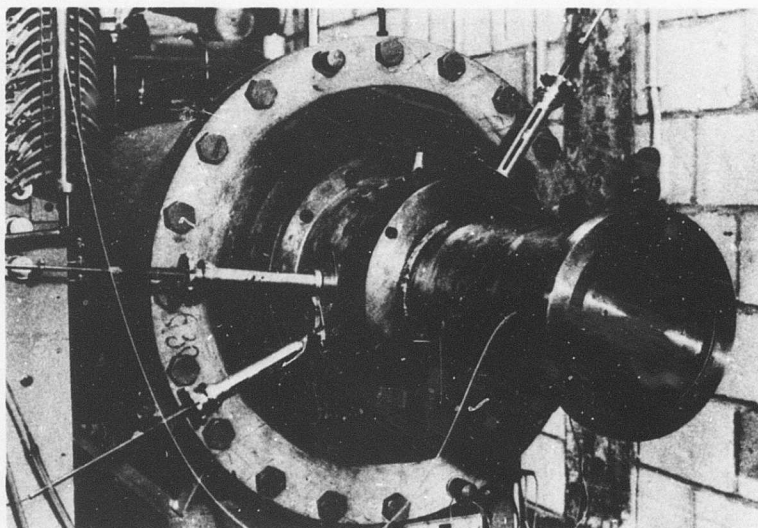


Figure 14. Stator Nozzle Test Rig.

3. Downstream total and directional (left-right) pressure.
4. Downstream total and directional (over-under) pressure.
5. Downstream static pressure.

Because of the very small exit flow area, every effort was made to minimize the probe blockage effect. This accounts for the avoidance of combination probes and for the contouring and minimum sections used in downstream probe construction. The probes were calibrated in the L-4 calibration duct located in the VKI laboratory.

TEST PROCEDURE

An attempt was made to simulate the actual flow design conditions by cold flow. Ideally, this would imply equivalent Mach numbers, equal Reynolds numbers, and similar ratios of specific heat (γ).

The latter is not consistent with cold flow simulation with air as the working fluid. However, the effect of unequal values of γ are small and can be neglected. The effect of nonequal Reynolds numbers can be small if the values are close and not in the critical range.

Therefore, primary importance was placed on obtaining equivalent Mach numbers. This was done by varying the inlet total pressure until the

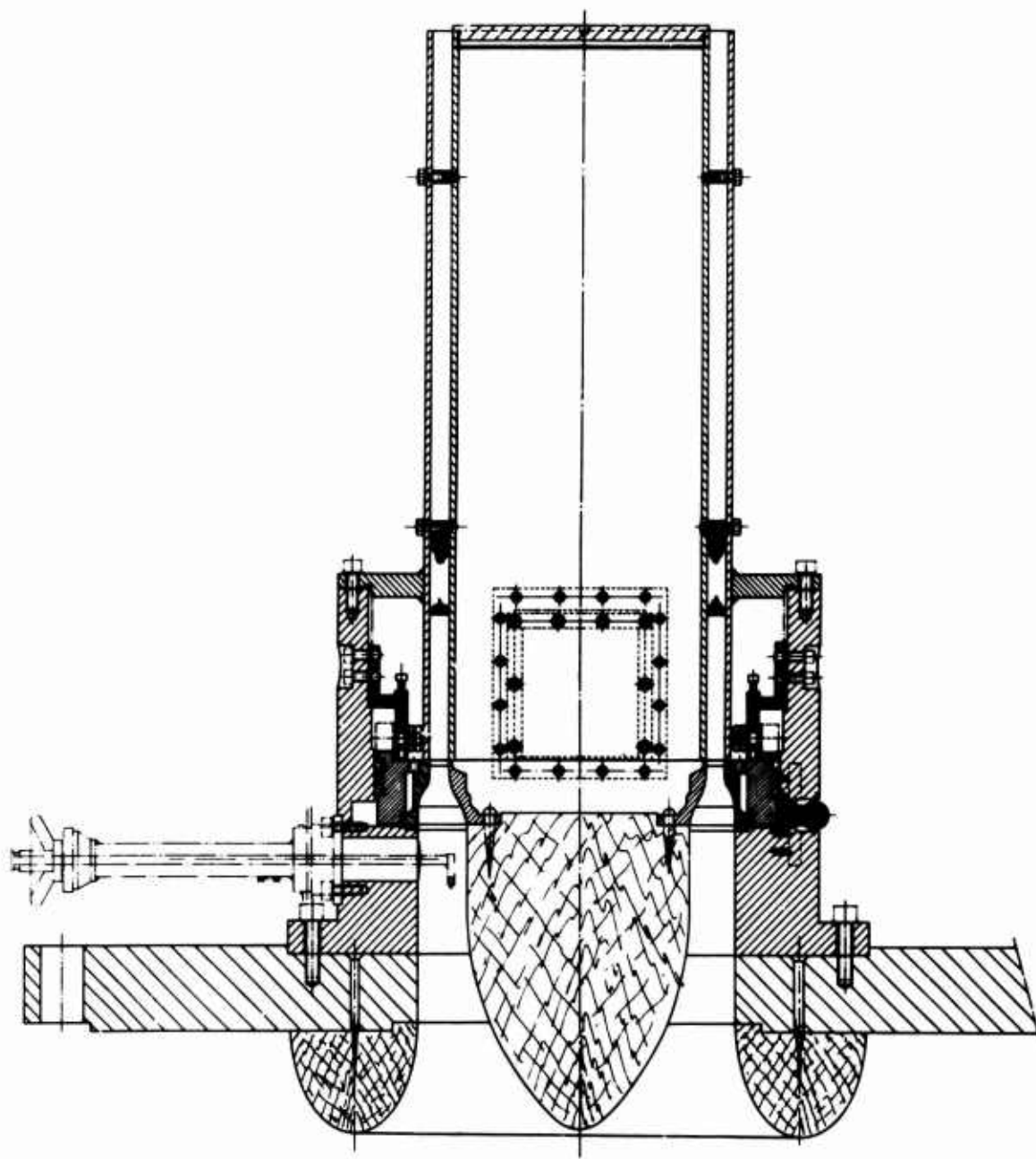


Figure 15. Stator Nozzle Test Rig.

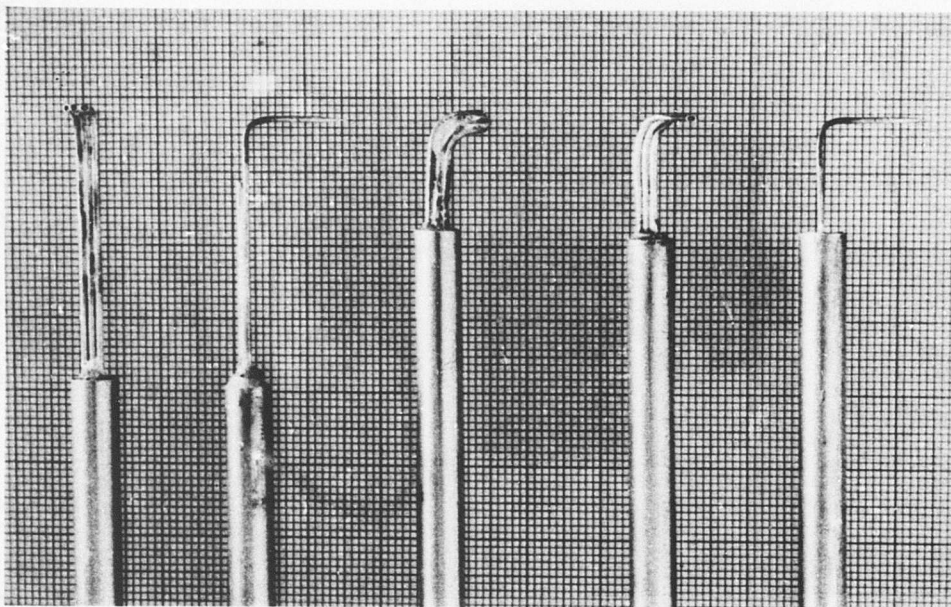


Figure 16. Stator Nozzle Test Probes.

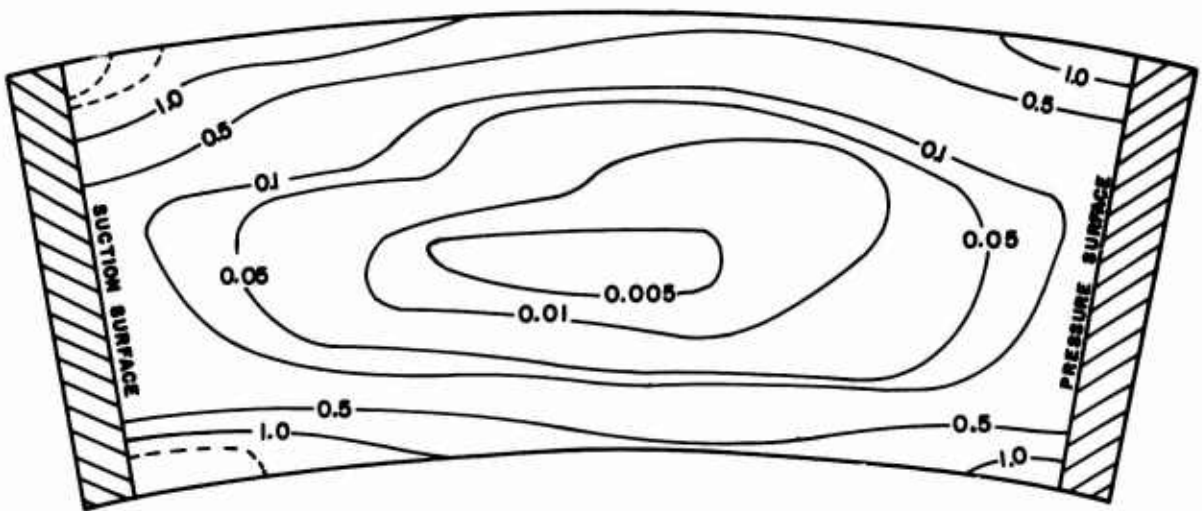
design value $M_2 = 1.0$ was obtained. The Mach number was calculated from downstream probe readings.

For design Mach number, circumferential traverses of static, total, and directional (left-right and over-under) pressures were made downstream at eight radial stations. A check of Reynolds number revealed that the cold flow value was slightly greater than the actual value and not near the critical range.

DISCUSSION OF RESULTS

Traverses of total and static pressure about 2 inches upstream of the model indicated no measurable differences from the settling chamber readings. This is reasonable, considering the very low inlet Mach number ($M_1 = 0.057$).

The loss variation at the stator nozzle outlet is given in Figure 17 in terms of coefficient $\bar{\omega} = P_{01} - P_{02} / P_{02} - P_2$, which is equivalent to Ainley's loss coefficient, Y . The existence of a separation vortex in the corners of the profile suction side and end walls is evident, indicating significant secondary flows. The apparent higher loss at the tip than at the hub is unusual for a three-dimensional cascade. It is believed that this is a result of the comparatively abrupt constriction on the nozzle outer wall.



$$\bar{\omega} = \frac{P_{01} - P_{02}}{P_{02} - P_2}$$

Figure 17. Stator Nozzle Outlet Loss Distribution, $\bar{\omega}$.

In Figure 18, the integrated radial variation of the stator loss is presented and represents a total experimental loss coefficient of $\bar{\omega} = .240$.

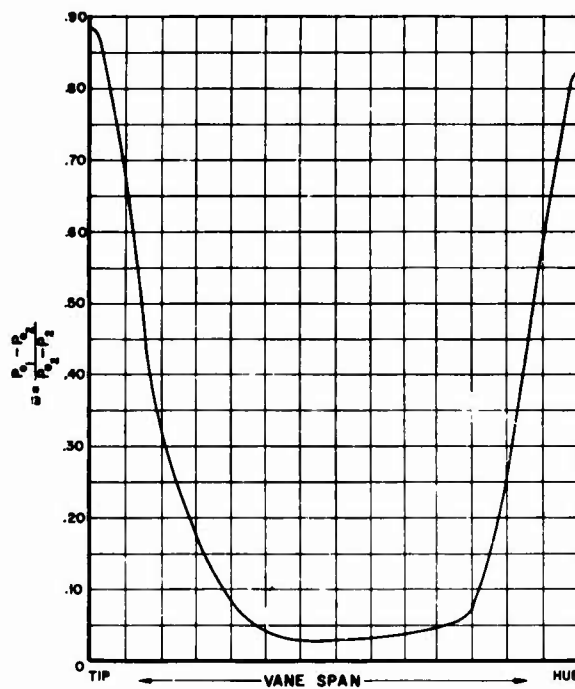


Figure 18. Radial Variation in Stator Nozzle Loss.

In Figure 19, the variation of nozzle outlet angle is shown both circumferentially and radially. The stator model designer appears to have not

taken into consideration the deviation angle, since both the camber and the deflection design values were 70 degrees. The average test outlet flow angle of 64.8 degrees indicates that a deviation of 5.2 degrees exists and should be considered in any future designs.

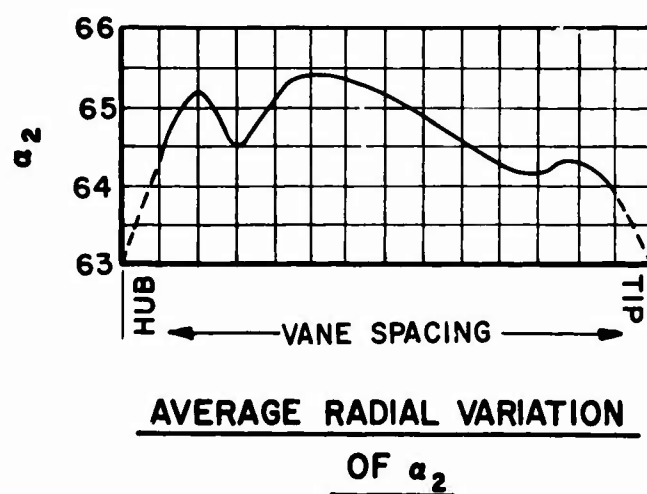
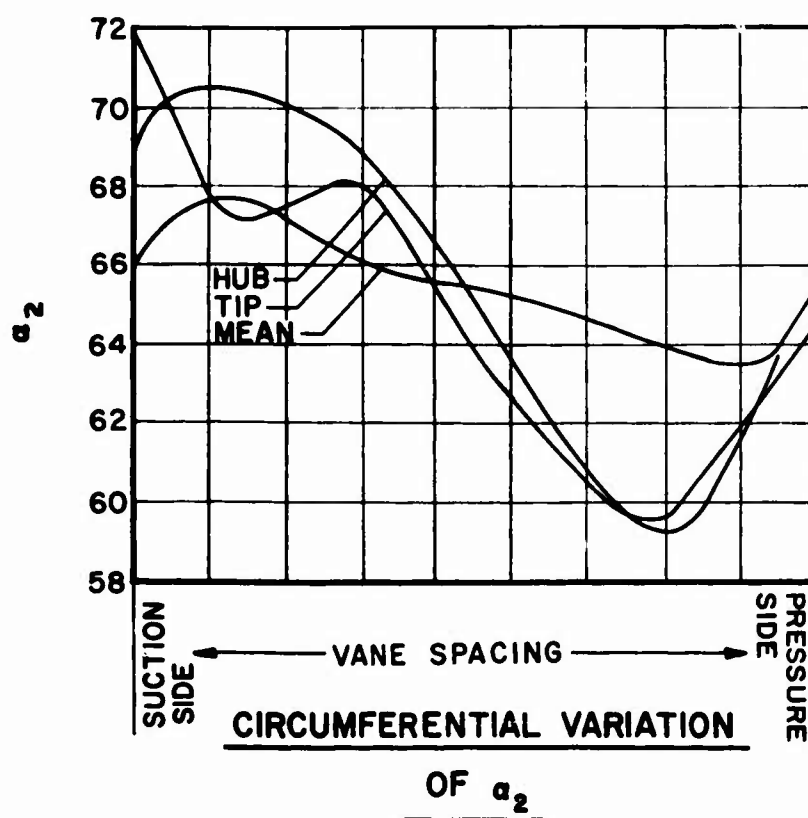


Figure 19. Variation of Stator Nozzle Outlet Angle, α_2 .

The experimental loss coefficient is based on a mass average of the flow through the channel. Although the probe readings in the corners of the profile suction surface and end walls are not accurate because of the existing separation vortex, it is believed that the effect on total performance is slight and that the previously quoted loss is of correct magnitude.

COMPARISON OF EXPERIMENTAL AND THEORETICAL LOSSES

Combining the loss predictions in terms of Soderberg's loss coefficient:

1. <u>Theoretical predictions</u>	
	ξ
Ainley	.0486
Soderberg	.1150
Markov	.1500
2. <u>Selected theoretical prediction</u>	
Soderberg + ξ_{TET}	.1414
3. <u>Experimental loss</u>	.1412

When these values are compared, it is obvious that experiment substantiated the selected prediction. Although the closeness of this match must be in part coincidence, it can be concluded that Soderberg's correlation as corrected by the author in a previous section of this report does provide an accurate performance prediction for a turbine stator of the loading and aspect ratio investigated.

The magnitude of the loss coefficient is also of significant interest, in that it indicates that for the low-aspect-ratio turbine stage, losses in the rotor are not much greater than those in the stator. Using Ainley's method, one would calculate a rotor loss to be about 250% of the stator loss. On the basis of this and other erroneous prediction methods, little effort has been advanced in the improvement of efficiency of the low-aspect-ratio turbine stage, the rationale being that significant increases in stage performance could be obtained only by significant decreases in rotor loss, which appeared to be unlikely. Furthermore, since stator losses were considered to be a relatively small portion of the overall loss, stator optimization was not considered to have a significant effect.

It is hoped that this report will have the effect of altering this viewpoint for the low-aspect-ratio turbine design and place the importance of stator performance in its true perspective.

LITERATURE CITED

1. White, J. W., ADVANCED ARMY COMPONENTS TECHNOLOGY PROGRAM, S. A. E. Preprint 650707, Combined Powerplant and Transportation Meeting, Cleveland, Ohio, 1965.
2. Gabel, Ronald M., and Tabbey, Arthur J., ADVANCEMENT OF HIGH-TEMPERATURE TURBINE TECHNOLOGY FOR SMALL GAS TURBINES — FLUID-COOLED AXIAL FLOW TURBINE, Continental Aviation and Engineering Corporation; USAAVLABS Technical Report 68-65, U. S. Army Aviation Materiel Laboratories, Fort Eustis, Virginia, January 1969, AD 686312.
3. Chauvin, J., THE INCREASE OF TURBINE INLET TEMPERATURES FOR SMALL GAS TURBINES: PERSPECTIVES AND PROBLEMS, von Kármán Institute TM 19, 1967.
4. Lakshminarayana, B., and Horlock, J. H., REVIEW: SECONDARY FLOWS AND LOSSES IN CASCADES AND AXIAL FLOW TURBOMACHINES, International Journal of Mechanical Sciences, Pergamon, Vol. 5, pp. 287-307, 1963.
5. New, W. R., AN INVESTIGATION OF ENERGY LOSSES IN STEAM TURBINE ELEMENTS BY IMPACT TRAVERSE STATIC TEST WITH AIR AT SUBACOUSTIC VELOCITIES, ASME Transactions, Vol. 62, pp. 489-502, 1940.
6. Deich, M. E., A NEW METHOD OF PROFILING THE GUIDE CASCADES OF STAGES WITH SMALL RATIOS OF DIAMETER TO LENGTH, Associated Electrical Industries (Manchester) Ltd, Translation n° 3277, 18 July 1963.
7. Deich, M. E., METHOD OF INCREASING THE EFFICIENCY OF TURBINE STAGES WITH SHORT BLADES, Associated Electrical Industries (Manchester) Ltd, Translation n° 2816, 29 April 1960.
8. Stewart, W. L., Whitney, W. J., and Wong, R. Y., A STUDY OF BOUNDARY LAYER CHARACTERISTICS OF TURBOMACHINE BLADE ROWS AND THEIR RELATION TO OVERALL BLADE LOSS, Journal of Basic Engineering, ASME Transactions, Vol. 82-D, p. 588, 1960.

9. Horlock, J. H., AXIAL FLOW TURBINES, FLUID MECHANICS AND THERMODYNAMICS, Butterworth & Co Ltd, 1966.
10. Ainley, D. G., and Mathieson, G. C. R., A METHOD OF PERFORMANCE ESTIMATION FOR AXIAL FLOW TURBINES, ARC R & M, 2974, 1957.

Unclassified

Security Classification

DOCUMENT CONTROL DATA - R & D		
<small>(Security classification of title, body of abstract and indexing annotation must be entered when the overall report is classified)</small>		
1. ORIGINATING ACTIVITY (Corporate author) U. S. Army Aviation Materiel Laboratories Fort Eustis, Virginia		2a. REPORT SECURITY CLASSIFICATION Unclassified 2b. GROUP
3. REPORT TITLE INVESTIGATION OF FACTORS AFFECTING SMALL TURBINE EFFICIENCY AND LOSS PREDICTION		
4. DESCRIPTIVE NOTES (Type of report and inclusive dates) Final Report		
5. AUTHOR(S) (First name, middle initial, last name) LeRoy T. Burrows		
6. REPORT DATE June 1969	7a. TOTAL NO. OF PAGES 40	7b. NO. OF REFS 10
8a. CONTRACT OR GRANT NO. NA 8b. PROJECT NO. Task 1G162203D14413 c. d.	9a. ORIGINATOR'S REPORT NUMBER USAAVLABS Technical Report 69-54 9b. OTHER REPORT NUM (Any other numbers that may be assigned this report)	
10. DISTRIBUTION STATEMENT This document is subject to special export controls and each transmittal to foreign governments or foreign nationals may be made only with prior approval of US Army Aviation Materiel Laboratories, Fort Eustis, Virginia 23604.		
11. SUPPLEMENTARY NOTES		12. SPONSORING MILITARY ACTIVITY U. S. Army Aviation Materiel Laboratories Fort Eustis, Virginia
13. ABSTRACT The aerodynamics and mechanics of the high-temperature, low-mass-flow, low- aspect ratio, axial-flow turbine are discussed. The problems of small size and resulting high secondary losses are considered, and approaches to improving efficiency are offered. In addition, experimental analysis of a turbine stator annulus (aspect ratio = 0.5) is presented, with recommendation for an accurate prediction of the losses in the small, high-performance turbine.		

DD FORM 1473

REPLACES DD FORM 1473, 1 JAN 64, WHICH IS
OBSOLETE FOR ARMY USE.

Unclassified

Security Classification

